Massive Stars Across Redshifts in the Era of JWST and Large Surveys
Proceedings IAU Symposium No. 402, 2026
A. Wofford, N. St Louis, M. García, S. Simón-Díaz & L. M. Oskinova, eds.
doi:10.1017/S1743921325103979

How protostellar jets remove angular momentum during the formation of massive stars

André Oliva[1,2], Sylvia Ekström[2], Patrick Eggenberger[2] and Georges Meynet[2]

[1]Space Research Center (CINESPA) and School of Physics, University of Costa Rica, Ciudad Universitaria Rodrigo Facio, 11501 San José, Costa Rica
email: astro@gandreoliva.org

[2]Département d'Astronomie, Université de Genève, Chemin Pegasi 51, 1290 Versoix, Switzerland

Abstract. Massive stars start their lives surrounded by accretion disks and launching powerful protostellar jets that carry mass and angular momentum away. For a long time, the exact mechanism that drives early protostellar jets was unknown. Using water maser observations obtained through very long-baseline interferometry in the star-forming region IRAS 21078+5211 and new detailed simulations, the launching mechanisms of the jet have been recently uncovered. In this contribution, we present these simulations (which include self-gravity, resistivity and radiation transport) and a comparison between the streamlines predicted by the simulations and the observed water maser patterns. As a result, we conclude that protostellar jets are launched magneto-centrifugally. We discuss how protostellar jets can remove angular momentum from the protostar, helping us uncover the origin of rotation on massive stars upon their arrival into the main sequence.

Keywords. Stars: massive, Stars: formation, Stars: pre-main sequence, Stars: rotation, ISM: jets and outflows

1. Introduction

During their formation, massive protostars become surrounded by accretion disks that deliver mass and angular momentum to them, and launch powerful magnetically-driven jets and outflows. The launching mechanism of the earliest protostellar jets has been uncovered thanks to recent water maser observations made through the technique of very long-baseline interferometry (VLBI) presented in Moscadelli et al. (2022), Moscadelli et al. (2023) and Moscadelli et al. (2024). As part of the *Protostellar Outflows at the Earliest Stages* (POETS) survey, the innermost ~ 100 au of the protostellar jet within the massive star-forming region IRAS 21078+5211 were examined. Thanks to the observed spatial patterns and kinematics of the water masers and a comparison against simulations presented in Oliva and Kuiper (2023b), Moscadelli et al. (2024) concluded that the flow is launched by a magnetohydrodynamical (MHD) disk wind mechanism similar to the classical model of Blandford and Payne (1982).

One open question from those studies was, how much angular momentum is the MHD jet removing and what impact it might have in the rotation rate of the protostar? In

© The Author(s), 2026. Published by Cambridge University Press on behalf of The International Astronomical Union. This is an Open Access article, distributed under the terms of the Creative Commons Attribution-NonCommercial-ShareAlike licence (https://creativecommons.org/licenses/by-nc-sa/4.0/), which permits non-commercial re-use, distribution, and reproduction in any medium, provided the same Creative Commons licence is used to distribute the re-used or adapted article and the original article is properly cited. The written permission of Cambridge University Press or the rights holder(s) must be obtained prior to any commercial use.

https://doi.org/10.1017/S1743921325103979 Published online by Cambridge University Press

this work, we start examining this question by taking one of the jet simulations used previously for comparison against IRAS 21078+5211 (Section 2) and then using it to build a prescription for the spin-down torque it produces onto a forming massive star (Section 3). In Section 4, we present our early results for the evolution of the surface angular velocity of an accreting protostar.

2. Jet *ab-initio* simulations

The jet simulation starts from the gravitational collapse of a molecular cloud core that contains 100 $M_\odot$ within 0.1 pc in slow solid-body rotation (the rotational to gravitational energy ratio is 4%). The cloud is initially threaded by a uniform magnetic field of 68.31 μG parallel to the rotation axis. The initial density is set following a power law $\rho \propto r^{-1.5}$.

The weakly ionized gas is modeled as a single fluid with the methods of magneto-hydrodynamics using the `Pluto` code (Mignone et al. 2007). Self-gravity and radiation transport (using gray flux-limited diffusion) are included thanks to the modules `Haumea` and `Makemake` respectively (Kuiper et al. 2020). Ohmic dissipation is considered as a non-ideal MHD effect using the formula by Machida et al. (2007). For details about the spatial grid utilized and the boundary conditions, we refer the reader to Oliva and Kuiper (2023a,b). We highlight here that the computational domain has an inner boundary of 3 au and extends until $r = 0.1$ pc, and that we use axial and equatorial symmetry. The computation is halted after 30 kyr of evolution, that is, our focus are the early stages of star formation, before stellar feedback (photoionization and radiation pressure) from the young massive star are considerable.

After an initial phase where the gravitational collapse dominates the kinematics ($t \lesssim 5$ kyr), enough angular momentum is transported towards the center of the cloud for a Keplerian-like accretion disk to form. The magnetic field is dragged by the gravitational collapse towards the center of the cloud, so the magnitude of the magnetic field increases towards the center as well. Roughly at the same time as the disk appears, magnetically-driven outflows form self-consistently along the rotation axis (i.e., they are not artificially injected in the simulation). The protostar is thus accreting mass and angular momentum through the disk and the magnetically driven outflows carry away a fraction of the mass and angular momentum that otherwise would reach the protostar.

The analysis of this simulation was presented in Oliva and Kuiper (2023b), where two kinds of magnetically-driven outflows were found: a tower flow and a jet. As the material collapses in the cloud, the magnetic field lines become increasingly twisted by rotation. The tower flow is driven by the magnetic pressure gradient that arises from the winding of magnetic field lines, has typical velocities of 10 km s^{-1}, and extends at large scales (1000–20 000 au) A fast jet (speed $\gtrsim 100$ km s^{-1}) also forms in the innermost ~ 100 au away from the protostar. This fast jet is launched magneto-centrifugally (see Sect. 3).

3. Angular momentum transported by the jet

The magneto-centrifugal jet is launched as follows: when the magnetic pressure gradient drives the magnetic tower flow, it opens a cavity. In the innermost ~ 100 au of the cavity, the density is very low, and the magnetic field is very strong (because the magnetic field lines are dragged to the center by the gravitational collapse). Both factors cause the Alfvén speed ($v_A = B/\sqrt{4\pi\rho}$) to increase, eventually becoming larger than the flow velocity (i.e., the flow becomes sub-Alfvénic). In this regime, the flow is in effect guided by the magnetic field lines. The material from the surface of the inner disk is lifted by the magnetic field and brought out of the gravito-centrifugal equilibrium. As the ejecta move to a larger orbit, they are simultaneously guided away from the protostar by the magnetic field, resulting in a conic helical motion.

https://doi.org/10.1017/S1743921325103979 Published online by Cambridge University Press

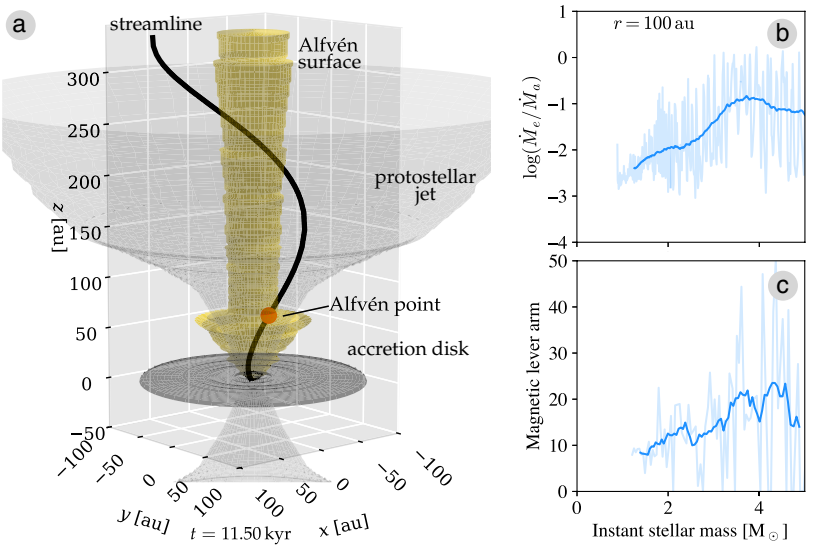


Figure 1. Disk-jet *ab-initio* simulations. (a) Streamline of the velocity co-rotating with the launching point, which inside of the Alfvén surface also coincides with a magnetic field line. The light gray surface is taken at a density of $10^{-16}\,\mathrm{g\,cm^{-3}}$ and the dark gray surface is taken at $10^{-13}\,\mathrm{g\,cm^{-3}}$. (b) Accretion to ejection rate taken at a fixed radius of 100 au. (c) Magnetic lever arm calculated for streamlines originating at $R_l \approx 100\,\mathrm{R}_\odot$.

The jet carries away mass and angular momentum as follows. In Fig. 1, we present the calculation of a streamline of the jet in the frame of reference that co-rotates with the launching point (located in this particular example at $R_l = 3$ au). Inside of the Alfvén surface (in yellow), the flow is sub-Alfvénic, thus the streamline also traces a magnetic field line. After crossing the Alfvén surface through the Alfvén point, the flow becomes super-Alfvénic, meaning that the ejecta becomes capable of dragging the flux-frozen magnetic field lines. This process enables the transfer of angular momentum from small to large scales.

We assume that the jet is capable of removing angular momentum from the surface of the forming star in a similar way than a magnetized stellar wind according to Weber and Davis (1967),

$$\frac{dJ_\star}{dt} \sim \Omega_\star R_A^2 \dot{M}_e \tag{1}$$

where $\Omega_\star$ is the surface angular velocity of the protostar, R_A is the cylindrical radius of the Alfvén point, and $\dot{M}_e$ is the mass ejected through the Alfvén surface. Following this assumption, we compute the last two factors of Eq. 1 from our jet simulations, the result of which is displayed in Fig. 1b and 1c. The ratio of the ejected mass to the accreted mass $\dot{M}_e/\dot{M}_a$ (Fig. 1b) was estimated by integrating the mass outflow and dividing it over the mass inflow within a sphere of 100 au. The magnetic lever arm (Fig. 1c) is defined as R_A/R_l and we estimated it by computing the Alfvén point of the streamline launched from the closest possible radius to the protostar within the limitations of the spatial resolution of our simulation ($R_l \approx 100\,\mathrm{R}_\odot$).

4. Protostellar rotation

We computed the pre-main sequence evolution of a rotating and accreting massive protostar using the Geneva stellar evolution code (Eggenberger et al. 2008) at solar

https://doi.org/10.1017/S1743921325103979 Published online by Cambridge University Press

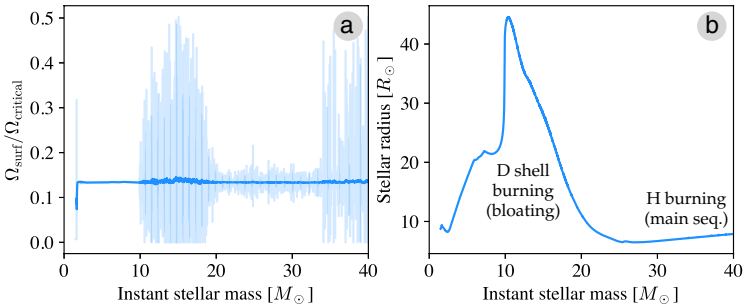


Figure 2. Evolution of the (a) surface rotation rate as a ratio of the critical value (b) evolution of the stellar radius. Because the accretion rate is fixed to a constant value of $5 \cdot 10^{-4}\,\mathrm{M}_\odot\,\mathrm{yr}^{-1}$, the instant stellar mass is a proxy for time. The darker blue curve on panel (a) is a running average.

metallicity. Motivated by the results of our jet simulation, we chose a constant accretion rate of $\dot{M}_a = 5 \cdot 10^{-4}\,\mathrm{M}_\odot\,\mathrm{yr}^{-1}$. In addition to considering mass and angular momentum accretion via a Keplerian-like accretion disk (Haemmerlé et al. 2016; Haemmerlé et al. 2017), we modified the code to include the spin-down torque of Eq. 1. Utilizing the data in Fig. 1b and 1c, we chose the values $\dot{M}_e = 0.05\dot{M}_a$ and $R_A = 20R_l \equiv 20R_\star$ to parametrize the jet.

The result of this experiment is shown in Fig. 2: as the protostar accretes, the surface angular velocity remains a constant ratio of the critical speed $\Omega_{\rm critical} = \sqrt{GM_\star/R_\star^3}$. This ratio is constant despite the strong changes in the protostellar structure (Fig. 2b), meaning it is independent on the mechanisms for internal angular momentum redistribution as the star undergoes through fully convective phases (before deuterium shell burning) or fully radiative phases (bloating phase), and even after the arrival onto the main sequence. Although the ratio $\Omega_\star/\Omega_{\rm critical}$ is constant, the angular velocity does change as a function of time as the star accretes, expands and contracts. However, because the jet torque depends on $\Omega_\star$, if the star spins up, the jet becomes more efficient in removing angular momentum, which brings the system to an equilibrium.

In this scenario, the angular velocity of the star will depend only on the properties of the jet, and those in turn depend on the initial conditions for star formation (as discussed in Oliva and Kuiper 2023b). This model will be discussed in more detail in an upcoming article. Our preliminary results are compatible with the accretion-powered wind scenario explored for low-mass star formation in, e.g., Matt and Pudritz (2005); Gallet et al. (2019); Gehrig and Vorobyov (2023).

References

Blandford, R. D. & Payne, D. G. 1982, *MNRAS*, 199, 883–903.
Eggenberger, P., Meynet, G., Maeder, A., Hirschi, R., Charbonnel, C., Talon, S., & Ekström, S. 2008, *Ap&SS*, 316(1-4), 43–54.
Gallet, F., Zanni, C., & Amard, L. 2019, *A&A*, 632, A6.
Gehrig, L. & Vorobyov, E. I. 2023, *A&A*, 673, A54.
Haemmerlé, L., Eggenberger, P., Meynet, G., Maeder, A., & Charbonnel, C. 2016, *A&A*, 585, A65.
Haemmerlé, L., Eggenberger, P., Meynet, G., Maeder, A., Charbonnel, C., & Klessen, R. S. 2017, *A&A*, 602, A17.
Kuiper, R., Yorke, H. W., & Mignone, A. 2020, *ApJS*, 250(1), 13.
Machida, M. N., Inutsuka, S.-i., & Matsumoto, T. 2007, *ApJ*, 670(2), 1198–1213.
Matt, S. & Pudritz, R. E. 2005, *ApJ*, 632(2), L135–L138.

https://doi.org/10.1017/S1743921325103979 Published online by Cambridge University Press

Mignone, A., Bodo, G., Massaglia, S., Matsakos, T., Tesileanu, O., Zanni, C., & Ferrari, A. 2007, *ApJS*, 170(1), 228–242.
Moscadelli, L., Oliva, A., Sanna, A., Surcis, G., & Bayandina, O. 2024, *A&A*, 690, A81.
Moscadelli, L., Oliva, A., Surcis, G., Sanna, A., Beltrán, M. T., & Kuiper, R. 2023, *A&A*, 680, A107.
Moscadelli, L., Sanna, A., Beuther, H., Oliva, A., & Kuiper, R. 2022, *Nature Astronomy*, 6, 1068–1076.
Oliva, A. & Kuiper, R. 2023,a *A&A*, 669a, A80.
Oliva, A. & Kuiper, R. 2023,b *A&A*, 669b, A81.
Weber, E. J. & Davis, Jr., L. 1967, *ApJ*, 148, 217–227.

https://doi.org/10.1017/S1743921325103979 Published online by Cambridge University Press